MADRID
inter.noise 2019
June 16 - 19
NOISE CONTROL FOR A BETTER ENVIRONMENT

On the sound absorption performance of corrugated micro-perforated panel absorbers

Wang, Chunqi[1,2] Liu, Xiang[1,2] Lixi, Huang[1,2]

[1)]**Lab of Aerodynamics and Acoustics, HKU-Zhejiang Institute of Research and Innovation, Lin An, 311305, Zhejiang, China**

[2)]**Department of Mechanical Engineering, The University of Hong Kong, Pokfulam Road, Hong Kong, China**

ABSTRACT

As an attractive alternative to traditional porous materials, micro-perforated panel (MPP) absorbers have been widely used in room acoustics, environmental noise remediation and duct noise control. In the previous works, the MPP is usually assumed to be a flat panel perforated with sub-millimeter orifices, and that is also the most common form of MPPs used in practice. In practice, however, corrugated panels are widely used in architecture as roofs, ceilings and walls not only for decoration but also for greater rigidity in comparison to the plane plates. For noisy environments such as swimming pools, perforated corrugated panels with a back sound absorption layer or corrugated micro-perforated panels (corrugated MPPs) can be conveniently used to achieve a favourable acoustic environment and reduce the noise level. So far, however, almost all reported studies on MPP absorbers are based on flat MPPs, and a comprehensive investigation on corrugated MPP absorbers is seldom seen. The main purpose of the present work is to investigate the sound absorption performance of corrugated MPP absorbers, with emphasis on comparison with that of flat MPP absorbers. To this end, a three-dimensional (3D) finite element model is established to simulate the sound absorption performance of the corrugated MPP absorber. The corrugated profile is assumed to be sinusoidal and other possible shapes such as triangle and trapezoid are excluded at the current stage. Results show that , replacing the flat MPP with a corrugated one modify the coupling mode in the air-mass system, resulting in different sound absorption performance in comparison with the conventional flat MPP absorbers.

Keywords: Micro-perforated panel, Corrugated, Sound absorption
I-INCE Classification of Subject Number: 35, 51

1. INTRODUCTION

As an attractive alternative to traditional porous materials, micro-perforated panel (MPP) absorbers have been widely used in room acoustics, environmental noise remediation and duct noise control. An MPP absorber can be simply constructed by fitting an MPP in front of a rigid backing wall. The MPP can be manufactured from various materials such as wood, metal, plastics and films, thus, the MPP absorber (MPPA) may

[1] cqwang@hku.hk; chunqi76@gmail.com

be used either in ordinary indoor conditions or in harsh and corrosive environment. Due to its promising potential, many efforts have been made to further improve or optimize the acoustic performance of MPPA. Apart from the basic construction mentioned above, multi-layer configurations [1-5], parallel arrangement of different MPP absorbers [6-10] and serial-parallel hybrid arrangement [11] are proposed and investigated. To enhance the low frequency absorption performance, composite designs are proposed in which Helmholtz resonators [12], extended tubes [13] or shunted loudspeakers [14] are combined in tandem to the MPP absorbers. Moreover, there are also reports about employing the structural resonances of the perforated panel to improve its absorption performance at low frequencies [15-18]. In all these works, the MPP is assumed to be a flat panel perforated with sub-millimeter orifices, and it is also the most common form of MPPs used in industry practice.

The present study concerns the acoustic properties of MPPA in which the perforated panel is corrugated instead of being flat. To avoid confusion, this configuration is called 'corrugated MPPA', and the absorber with flat MPP is called 'flat MPPA' in the following. Corrugated panels are widely used in architecture as roofs, ceilings and walls not only for decoration but also for greater rigidity than the plane plates. For noisy environments such as swimming pools, perforated corrugated panels with a back sound absorption layer or corrugated MPP can be conveniently used to achieve a favourable acoustic environment and reduce the noise level. Besides, corrugated MPP is also proposed to be used in gas turbine systems for different sound attenuation properties compared with flat MPP [19]. So far, however, almost all reported studies on MPP absorbers are based on flat MPPs, and a comprehensive investigation on corrugated MPPA is seldom seen.

The main purpose of the present work is to investigate the sound absorption characteristics of corrugated MPPA, with emphasis on comparison with its flat counterpart. It is known that the sound absorption of MPP absorber is dominated by the mass-spring vibration system consisting of the air inside the micro-perforations (acoustic mass and damping) and the air gap between the MPP and the backing wall (spring) [1, 20]. Replacing the flat MPP with a corrugated one will inevitably alter the coupling in the mass-spring system, resulting in different sound absorption performance. So, it is of considerable interest to carry out a systematic study to elaborate the effects of corrugated profiles on the sound absorption of MPP absorbers.

In this paper, a three-dimensional (3D) numerical model is used to simulate the acoustic properties of the corrugated MPPA. The corrugated profile is assumed to be sinusoidal and other possible shapes such as triangle and trapezoid are excluded at the current stage. Results show that the absorption characteristics of corrugated MPPA can be very different from conventional flat MPPA. Efforts are made to analyse the absorption mechanism of the corrugated MPPA. The effect of different design factors are also examined.

2. Theoretical modelling

Fig. 1a shows schematically a sinusoidally corrugated panel with thickness h, corrugation pitch L and corrugation depth H_p. The corrugated panel is perforated with a series of submillimeter circular orifices (corrugated MPP) with diameter d, and the perforation ratio σ is defined as the percentage of the perforated area to the whole surface area of the MPP. The corrugated MPP is backed by an acoustically rigid wall with constant distance H_c away from the middle plane of the corrugated profile, which forms the so-called corrugated MPPA.

A 3D theoretical model as shown in Fig. 1(b) is used to describe the acoustic behaviors of the corrugated MPPA. The MPP is assumed to be infinitely large and only one period of the sinusoidal corrugated panel needs to be modelled for simplification, as shown in the *y* direction in Fig. 1(b). In this way, the air gap between the MPP and the rigid wall is represented by a backing cavity with cavity depth H_c. Periodic boundary conditions are required on the four sides of the backing cavity. The dimension in the x-direction is somewhat arbitrarily chosen to be half the corrugation pitch. When the normal incidence sound absorption performance is of interest, the 3D theoretical model can be reduced to a 2D one by neglecting the *x*-dimension in Fig. 1(b). The corrugated MPP is supposed to be rigid in this study, and the effect of structural vibration on sound absorption is excluded.

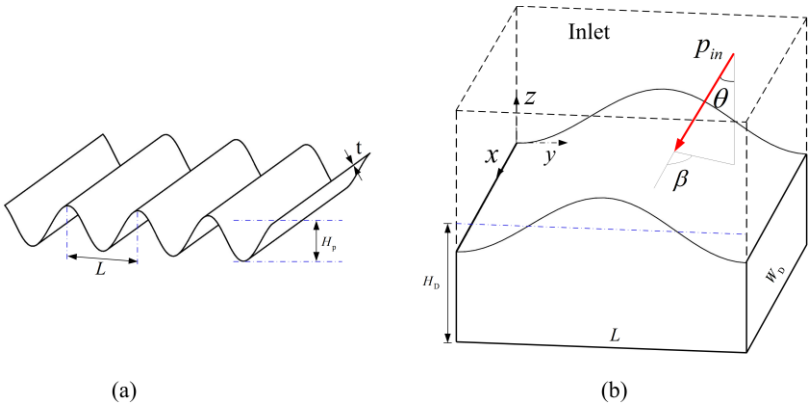

Figure 1: Overview of the corrugated MPPA. (a) Schematic of the corrugated panel; (b) Theoretical model of the MPPA under oblique incidence of sound waves. The dashed lines indicate the additional virtual duct for modeling the sound field outside the MPPA.

Suppose a plane sound wave p_{in} with unit amplitude is obliquely incident on the corrugated MPP with polar angle of θ and azimuthal angle of β,

$$p_{\text{in}} = \mathrm{e}^{\mathrm{i}[\omega t+(k_0 \sin\theta\cos\beta)x+(k_0 \sin\theta\sin\beta)y+(k_0\cos\theta)z]} \tag{1}$$

where ω is the angular frequency, $k_0 = \omega/c_0$ is the wavenumber in air, and $\mathrm{i} = \sqrt{-1}$ is the imaginary unit. The incident sound energy is partly reflected or scattered, and the rest is dissipated by the corrugated MPP. The acoustic impedance of the corrugated MPP is determined using Maa's formula for flat MPP [1],

$$Z = \frac{32\eta t}{\sigma\rho_0 c_0 d^2}\left[\left(1+\frac{K^2}{32}\right)^{1/2}+\frac{\sqrt{2}}{32}K\frac{d}{t}\right]+\mathrm{i}\frac{\omega t}{\sigma c_0}\left[1+\left(9+\frac{K^2}{2}\right)^{-1/2}+0.85\frac{d}{t}\right] \tag{2}$$

In the frequency domain, the 3D Helmholtz equation governs the sound field inside and outside the backing cavity,

$$\left(\frac{\partial^2}{\partial x^2}+\frac{\partial^2}{\partial y^2}+\frac{\partial^2}{\partial z^2}+k_0^2\right)p = 0 \quad . \tag{3}$$

On both sides of the corrugated MPP, the acoustical particle velocity in the normal direction to the local surface is given as,

$$u_{\mathbf{n}} = \frac{(p_{\text{cav}} - p_{\text{duct}})}{Z} \tag{4}$$

where **n** denotes the direction normal to the local surface; Z is defined in Equation (2), p_{cav} and p_{duct} are sound pressures on the cavity side and the virtual duct side respectively.

Finite element method is used to simulate the acoustic performance of the corrugated MPPA in the frequency domain. The computational domains include the backing cavity, the corrugated MPP and the virtual exterior duct, as shown in Fig. 1(b). Apart from the governing equation defined in Equation (3) and the continuity condition over the MPP surface, Equation (4), periodic boundary conditions are required on the four sides of the backing cavities and the virtual exterior ducts. Meanwhile, the reflected waves should be able leave the virtual inlet without any artificial reflections. In other words, a non-reflection boundary condition should be implemented at the inlet. A Dirichlet-to-Neumann (DtN) boundary condition [21] is implemented at the inlet of the virtual duct to emulate the non-reflection propagation of the reflected sound waves passing through the virtual inlet.

The Helmholtz equation (3) and relevant boundary conditions are solved using the finite element software package COMSOL Multiphysics®. The acoustic power dissipated by the corrugated MPP is then found as,

$$P_{\mathrm{abs}} = -\iint_{\mathbf{S}_{\mathrm{Inlet}}} \mathrm{Re}(p u_z^*)\mathrm{d}x\mathrm{d}y \tag{5}$$

where the asterisk denotes complex conjugate. With the incident sound wave p_{in} defined in Equation (1), the total acoustic power incident on the corrugated MPP surface is expressed as ,

$$P_{\mathrm{in}} = LW_{\mathrm{D}} \cos\theta / (\rho_0 c_0). \tag{6}$$

Therefore the absorption coefficient of the corrugated MPPA is found as the ratio of P_{abs} and P_{in},

$$\alpha_{\theta,\beta} = P_{\mathrm{abs}} / P_{\mathrm{in}} \tag{7}$$

When the polar angle θ=0, Equation (7) calculates the normal incidence absorption coefficient α_{N}.

3. RESULTS

The normal incidence absorption performance of the corrugated MPPA is investigated numerically. The following parameters are used as the default values,

L=50 mm, H_{p}=100 mm, H_{D}= 200 mm, W_{D}=25 mm

d=0.4 mm, t=0.4 mm, σ=1% (8)

where L, H_{p}, H_{D} and W_{D} define the geometrical configuration as shown in Fig. 1b, d, t and σ specify the properties of the micro-perforations. The choice of parameters in (8) is made somewhat arbitrarily, and no special effort is made to optimize the acoustic performance of the corrugated MPPA at the current stage.

3.1 Absorption characteristics

Fig. 2a compares the absorption characteristics of the corrugated and flat MPPAs. To make the comparison fair, the distance between the flat MPP and the rigid wall is also chosen as H_{D}=200 mm so that both the corrugated and flat MPPAs occupy the same backing cavity volumes. Two general observations can be made from Fig. 2a. First, for the given parameters, the absorption level of the corrugated MPPA is obviously decreased at the spectral peaks when compared with that of its flat counterpart. The reason for this performance decrease is analysed preliminarily by considering the actually larger

perforated area of the corrugated MPP than the flat MPP for the same incident plane. The bulk perforation ratio of the corrugated MPP is much higher than the nominal perforation ratio, σ=1%. As a result, the bulk acoustic resistance of the corrugated MPP is much smaller than that of the flat MPP, referring to Equation (2), and the insufficient acoustic resistance explains the lower sound absorption peaks of the corrugated MPPA shown in Fig. 2(a).

When the perforation ratio of corrugated MPP is chosen as σ=0.24%, the bulk perforation ratio can be calculated as σ'=1% with L=50 mm and H_p=100 mm. Results in Fig. 1b demonstrate that the corrugated MPP with σ=0.24% performs almost the same as the flat MPP with σ=1% in the low frequency range, say, below 800 Hz.

Another significant observation from Fig. 2 is that the sound absorption levels at the dips are considerably enhanced compared with the flat MPPA. It is a favourable property for reverberation control or broadband random noise reduction in large spaces and buildings. The present study shows that the modified coupling pattern between the acoustic modes and the MPP accounts for this performance improvement.

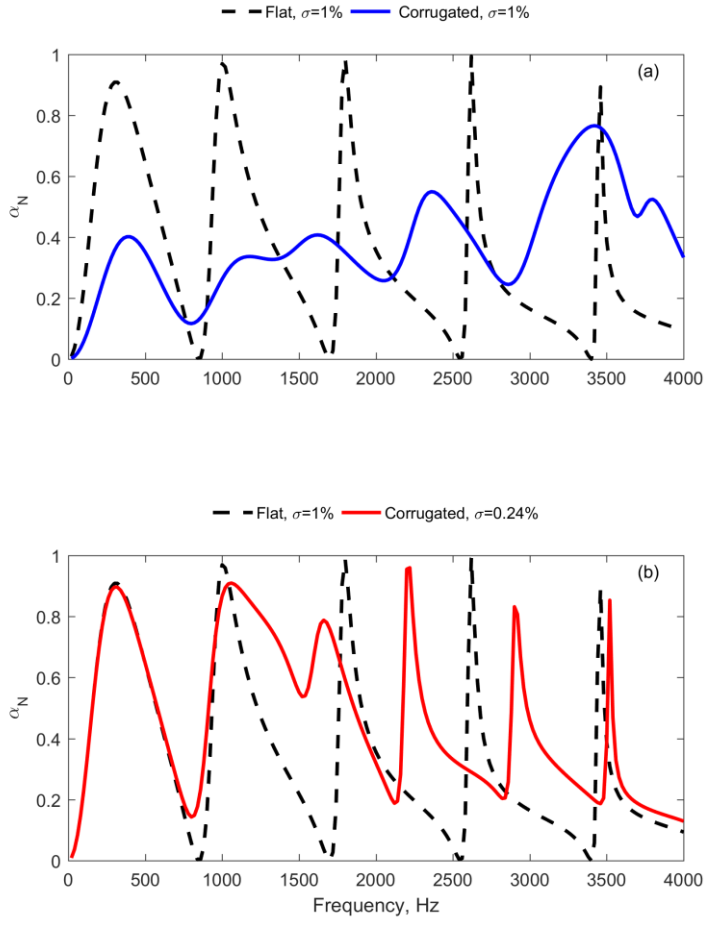

Figure 2: Comparison of normal incidence absorption coefficients between corrugated and flat MPPA. (a) $\sigma_{\text{Flat}} = \sigma_{\text{Corrugated}} = 1\%$ *(b)* $\sigma_{\text{Flat}} = \sigma'_{\text{Corrugated}} = 1\%$.

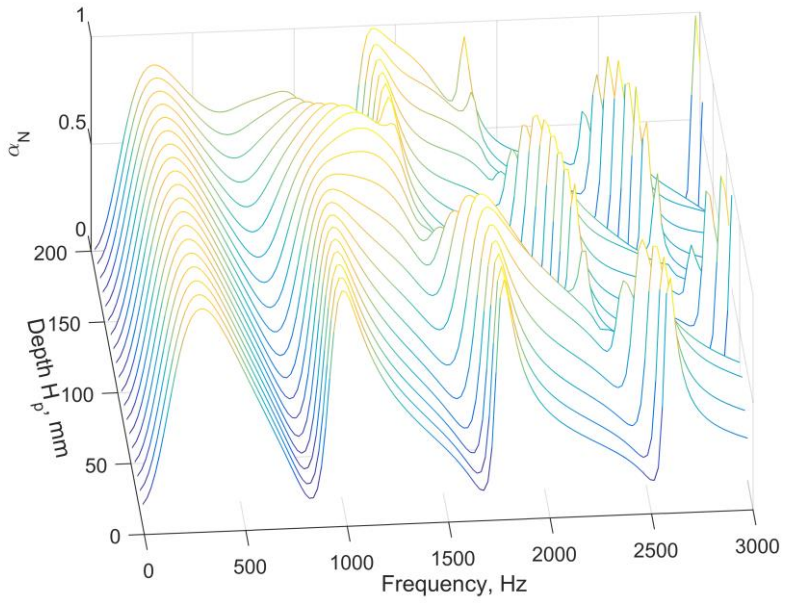

Figure 3: Variation of absorption performance of the corrugated MPPA with respect to corrugation depth. The corrugation pitch is fixed as L=50 mm. The bulk perforation ratio of the MPP is kept the same for all H_p.

The profile of the sinusoidal corrugated MPP can be completely determined by two factors: corrugation depth H_p and corrugation pitch L. The influence of the two factors on the absorption performance is investigated. Fig. 3 shows the variation of the normal incidence absorption coefficients with the corrugation depth. The corrugation pitch is fixed as L=50 mm. For a small corrugation depth H_p=20 mm, the absorption curve looks almost the same as that of the flat MPP absorber as shown in Fig. 2(a), except that the dip level (around 2500 Hz) is slightly raised. As H_p increases, the performance enhancement at off-resonance frequencies becomes more and more pronounced; and the absorption peaks move to lower frequencies. These influences due to corrugation also shift to lower frequencies as H_p increases. It is found that the influence of corrugation on sound absorption becomes significant when the corrugation depth is larger than quarter wavelength of the incident acoustic waves, $\lambda/4$. The corrugated MPP performs almost the same as the flat MPP when the corrugation depth is small compared with $\lambda/4$. The coincidence of the two absorption curves below 800 Hz in Fig. 2(a) just illustrates this relationship.

Fig. 4 shows the variation of the normal incidence absorption coefficients with the corrugation pitch raging from L=20 mm to L=100 mm. The corrugation depth is fixed at H_p= 100 mm. It can be seen that the change of absorption curves is trivial for different corrugation pitches, which is in sharp contrast to the dramatic change of absorption curves when the corrugation depth varies. In other words, the corrugation pitch is less influential than the corrugation depth on the absorption performance of the corrugated MPPA, although both factors weigh equally in determining the degree of corrugation

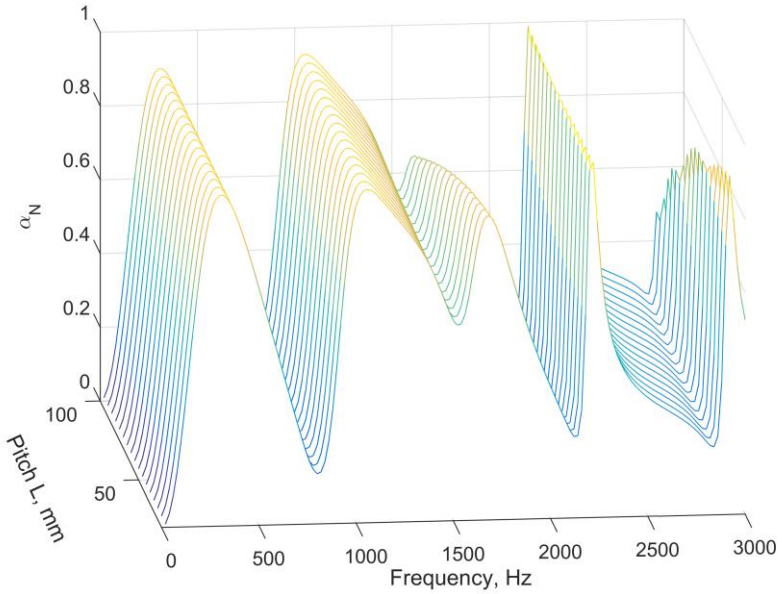

Figure 4: Variation of absorption performance of the corrugated MPPA with respect to corrugation pitch. The corrugation depth is fixed at H_p= 100 mm. The bulk perforation ratio of the MPP is kept the same for all L.

3.2 Acoustic modal analysis

The acoustic modes of the air gap between the MPP and the rigid backing wall are investigated and their contributions to the total sound absorption are analysed at the spectral peaks and dips of the absorption curve. For easy identification, the spectral peaks and dips are marked by P_1^F-P_5^F, P_1^C-P_6^C, D_1^F-D_4^F and D_1^C-D_5^C in Fig. 5. The superscripts 'F' and 'C' refer to flat and corrugated MPPs respectively.

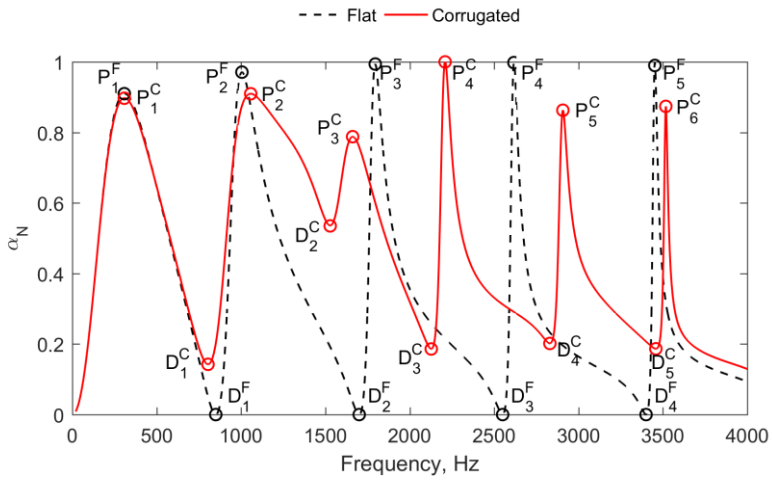

Figure 5: Comparison of absorption curves between corrugated and flat MPPA with spectral peaks and dips marked for easy identification. The bulk perforation ratios of the two configurations are kept the same as σ'=1%.

For the flat MPPA, the MPP and the backing wall define an air gap with constant thickness H_C (cf. Fig. 1) whose acoustic modes can be described analytically as,

$$\psi_n^F = \cos\left(n\pi z / H_D\right), \text{ with } n = 0,1,2,\cdots \text{ and } 0 \le z \le H_D \cdots, \quad (9)$$

and the corresponding resonance frequencies are $f_n^F = c_0/(2nH_D)$. For the corrugated MPPA, its acoustic modes and resonance frequencies are computed numerically using the finite element software COMSOL Multiphysics®. The calculated resonance frequencies are listed in Table 1. The mode shapes for corrugated configuration are shown in Fig. 6.

Table 1: The nonzero resonance frequencies of the air gap (Hz).

Mode No.	1	2	3	4	5	6
Flat MPP	850	1700	2550	3400	4250	5100
Corrugated MPP	806	1437	2124	2813	3462	4171

The air mass inside the perforations of the MPP and the backing air gap (spring) constitute a mass-spring vibration system. For the flat MPPA, the dips of the absorption curve, D_1^F-D_4^F, appear exactly at the resonance frequencies of the air gap, referring to Fig. 5 and Table 1. At the resonance frequencies, the stiffness of the air gap becomes infinity and the air mass is unable to vibrate through the perforations, hence no sound absorption occurs. On the other hand, maximum sound absorptions occur at the resonance frequencies of the mass-spring system, say, P_1^F-P_5^F. For the flat MPPA, only one acoustic mode is excited and contributes to the sound absorption at the resonance frequency [22]. Specifically, the sound absorption at P_1^F-P_5^F is exclusively dominated by the acoustic modes $\psi_0^F - \psi_4^F$ respectively. When the flat MPP is replaced by a corrugated one, the resonance frequencies of the air gap decrease. As shown in Table 1, the decrease of resonance frequency gets more and more significant as the order of acoustic modes increases. The spectral dips of the corrugated MPPA roughly agree with the corresponding resonance frequencies of the air gap. So, the overall spectral pattern also shifts to lower frequencies.

It is of interest to note that the absorption coefficients are considerably higher than zero at D_1^C-D_5^C in Fig. 5. The absorption coefficient is as high as $\alpha_N = 0.55$ at D_2^C. In contrast, the absorption coefficient of the flat MPPA vanishes completely at D_1^F-D_5^F. It is known that the absorption performance of the MPPA is determined by the dynamic response of the air mass-spring system. Therefore, the above comparison suggests that different vibro-acoustic coupling mechanism exists between the flat and corrugated MPPAs. To reveal this difference, the sound filed in the corrugated air gap is expanded in terms of the acoustic modes ψ_m^C,

$$p = \sum_m A_m \psi_m^C, \quad m = 0,1,\cdots \quad (10)$$

The magnitude of A_m measures the contribution of each mode ψ_m^C to the sound filedin the air gap. Due to the orthogonality property of the acoustic modes ψ_m^C, the amplitude of each mode can be evaluated as,

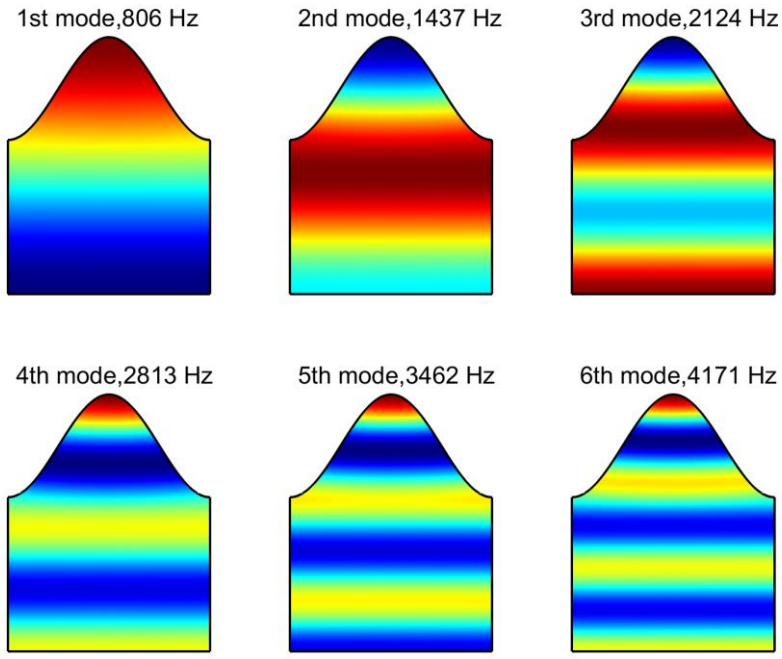

Figure 6: Nonzero acoustic modes of the air gap defined by the corrugated MPP and the rigid backing wall.

$$A_{\mathrm{m}} = \frac{\iiint_V p\hat{\psi}_{\mathrm{m}}^{C} dv}{\iiint_V \psi_{\mathrm{m}}^{C}\hat{\psi}_{\mathrm{m}}^{C} dv} \tag{11}$$

where V refers to the whole computational domain for the air gap, and ^ denotes complex conjugate. In this study, the sound filed p and acoustic modes $\psi_{\mathrm{m}}^{\mathrm{C}}$ are computed using finite element simulation, and Equation (11) is then evaluated through numerical integration.

Fig. 7 shows the normalized magnitude of each ψ_{m}^{C} in the total sound field at the first three peaks ($\mathrm{P}_1^{\mathrm{C}}$-$\mathrm{P}_3^{\mathrm{C}}$) and dips ($\mathrm{D}_1^{\mathrm{C}}$-$\mathrm{D}_3^{\mathrm{C}}$). There is one dominant acoustic mode at each peak or dip frequency, together with multiple adjacent acoustic modes that also contribute considerable to the sound filed. This multi-mode response of the corrugated configuration is different from the flat configuration in which only the resonating mode constitutes the sound field at the peak and dip frequencies. A plausible explanation for the multi-mode response is given below. The corrugated profile of the MPP causes a phase mismatch between the incident plane wave and the modal response inside the air gap across the MPP surface. As a result, acoustic modes other than the one in resonance may also be excited. At the dip frequency, the resonating acoustic mode inside the air gap still prevents the vibration of the air mass in the micro-perforations, just as in the flat MPPA. However, the non-resonating modes which also constitutes part of the total sound filed, allow the vibration of the air mass, and hence dissipation of acoustic energy through the viscous damping in the micro-perforations. The energy dissipation associated with the

non-resonating modes leads to the non-zero absorption coefficients at the dip frequencies of the corrugated MPPA.

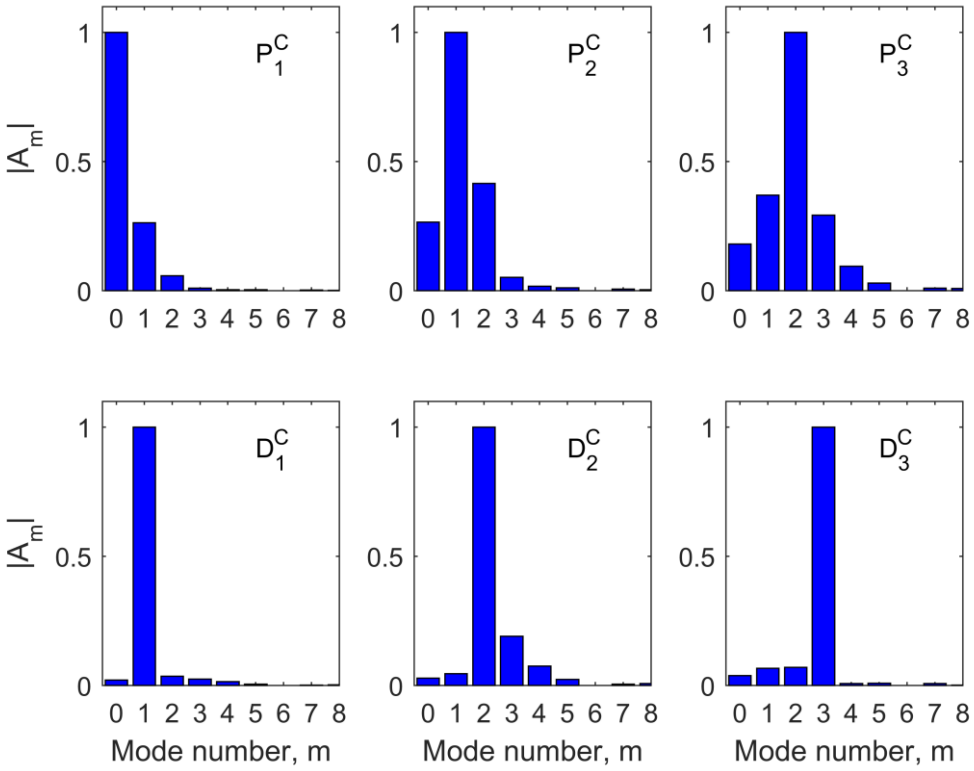

Figure 7: Amplitudes of the first nine modes in the corrugated MPPA at the spectral peaks (P_1^C-P_3^C) and dips (D_1^C-D_3^C). All amplitudes are normalized by the maximum amplitude at each frequency.

4. CONCLUSIONS

The acoustic performance of the corrugated MPPA is investigated and compared with the conventional flat MPPA. A 3D FE model is created to simulate the acoustic behavior of the corrugated MPPA. Numerical results show that the absorption characteristics of corrugated MPPA can be very different from conventional flat MPPA. The corrugation depth is found to be more influential than the corrugation pitch on the sound absorption. At high frequencies, the corrugation has a profound effect on the absorption properties of the corrugated MPPA. The absorption coefficients of the corrugated MPPA are considerably enhanced at the dips (anti-resonance frequencies) of the absorption curve, which is in sharp contrast to the zero absorption of the flat MPPA. This property is favorable for reverberation control or broadband random noise reduction in large spaces and buildings. Modal analysis shows that multiple modes of the corrugated configuration are excited at the peak and dip frequencies, and the acoustic response by the non-resonating modes give rise to the performance improvement of the corrugated MPPA.

5. ACKNOWLEDGEMENTS

This project is supported by National Natural Science Foundation of China (Grant No. 51775467).

6. REFERENCES

1. D.Y. Maa, “Micorperforated Panel wide-band absorber,” Noise Control Engineering Journal **29**, 77-84 (1987)
2. K. Sakagami, M. Yairi and M. Morimoto, “Multiple-leaf sound absorbers with microperforated panels: an overview” , Acoustics Australia 38 (2) , pp.76 - 81 , (2010)
3. T. Bravo, C. Maury and C. Pinhede, “Absorption and transmission of boundary layer noise through flexible multi-layer micro-perforated structures,” Journal of Sound and Vibration 395, 201-223, (2017)
4. D. Chang, F. Lu, W. Jin and B. Liu, “Low-frequency sound absorptive properties of double-layer perforated plate under grazing flow”, Applied Acoustics 130, 115-123, (2018).
5. F. Bucciarelli, GPM, Fierro and M. Meo, “A multilayer microperforated panel prototype for broadband sound absorption at low frequencies ”, Applied Acoustics 146, 134-144, (2019).
6. C.Q. Wang and L.X. Huang, “On the acoustic properties of parallel arrangement of multiple micro-perforated panel absorbers with different cavity depths,” Journal of the Acoustical Society of America 130 208-218, (2011)
7. D. Li, D. Chang and B. Liu, “Enhancing the low frequency sound absorption of a perforated panel by parallel-arranged extended tubes”, Applied Acoustics 102, 126-132 (2016)
8. H. Min and W. Guo, “Sound absorbers with a micro-perforated panel backed by an array of parallel-arranged sub-cavities at different depths”, Applied Acoustics 149, 123-128, (2019).
9. C.Q. Wang and Y.S. Choy, “Investigation of a compound perforated panel absorber with backing cavities partially filled with polymer materials”, Journal of Vibration and Acoustics, Transtions of the ASME 137(4), 044501, (2015).
10. C. Wang, C. Jiang and L. Huang, “Numerical investigation of the acoustic characteristics of ducts lined with poroelastic materials”, Proceedings of 46th International Congress and Exposition on Noise Control Engineering (INTER-NOISE 2017), Hong Kong, China, August 2017.
11. Y.J. Qian, J. Zhang, N. Sun, D.Y. Kong and X.X. Zhang, “Pilot study on wideband sound absorber obtained by adopting a serial-parallel coupling maner”, Applied Acoustics 124, 48-51, (2017)
12. S.H. Park, A design method of micro-perforated panel absorber at high sound pressure environment in launcher fairings. Journal of Sound and Vibration 332 (2013) 521-535.
13. D. Li, D. Chang and B. Liu, “Enhanced low-to mid-frequency sound absorption using parallel-arranged perforated paltes with extended tubes and porous material”, Applied Acoustics 127, 316-323, (2017).
14. J. Tao, R. Jing and X. Qiu, “Sound absorption of a finite micro-perforated panel backed by a shunted loudspeaker”, Journal of the Acoustical Society of America 135(1), 231-239, (2014).
15. S.W. Ren, L. Van Belle, C. Claeys, F.X. Xin, T.J. Lu, E. Deckers and W. Desmet, “Improvement of the sound absorption of flexible micro-perforated panels by local resonances”, Mechanical Systems and Signal Processing 117, 138-156, (2019).
16. D. Chang, B. Liu and X. Li, “An electromechanical low frequency panel sound absorber,” Journal of the Acoustical Society of America **128**, 639-645 (2010).

17. Y.Y. Lee, E.W.M. Lee and C.F. Ng, “Sound absorption of a finite flexible micro-perforated panel backed by an air cavity,” Journal of Sound and Vibration **287**, 227-243 (2005).
18. T. Bravo, C. Maury, C. Pinhede, “Sound absorption and transmission through flexible micro-perforated panels backed by an air layer and a thin plate”, Journal of the Acoustical Society of America 131(5), 3853-3863, (2012).
19. E.Y. Fung, R. L. Loud, V. Ponyavin, D. Venugopal, D. Nowak and M. Bialkowski, “System and method for fluid acoustic treatment”, US Patent 20180135515.
20. D.Y. Maa, “Potential of microperforated panel absorber,” Journal of the Acoustical Society of America **104**, 2861-2866 (1998).
21. C. Wang, L. Huang, Y. Zhang, “Oblique incidence sound absorption of parallel arrangement of multiple micro-perforated panel absorbers in a periodic pattern”， Journal of Sound and Vibration 333,6828-6842, (2014)
22. C. Wang, L. Cheng, J. Pan and G. Yu, “Sound absorption of a micro-perforated panel backed by an irregular-shaped cavity”, Journal of the Acoustical Society of America 127, 238-246, (2010)